C.P. No. 694

C.P. No. 694

MINISTRY OF AVIATION

AERONAUTICAL RESEARCH COUNCIL

CURRENT PAPERS

Boundary Layer Characteristics of Caret Wings

by

D. Catherall

LONDON: HER MAJESTY'S STATIONERY OFFICE

1963

PRICE 7s 6d NET

U.D.C. No. 533.693.3 : 532.526

C.P. No. 694

May, 1963

BOUNDARY LAYER CHARACTERISTICS OF CARET WINGS

by

D. Catherall

SUMMARY

The theory of laminar boundary layers along flat surfaces has been used in conjunction with Eckert's "Intermediate Enthalpy" method to obtain approximations to the displacement thickness, skin friction and temperature profiles on the undersurface of a Caret wing configuration. To a first approximation it has been assumed that parallel flow exists behind the shock outside the boundary layer, and the displacement of the shock by the boundary layer near the leading edge is neglected.

Conduction of heat within the body and along the surface is neglected, but radiation is included, so that 'local' values of equilibrium temperature are found. Examples are given for various altitudes and configurations and the effect of the skin friction on the lift/drag ratio calculated, assuming the undersurfaces to be plane.

Replaces R.A.E. Tech Note No. Aero 2835 - A.R.C. 24,222.

LIST OF CONTENTS

LIST OF ILLUSTRATIONS

1 INTRODUCTION

Nonweiler[1] and Maikopar[2] have both remarked that under certain conditions a plane shock can be made to lie across the underside of a delta wing with an inverted 'V' cross-section and that behind the shock (except in the boundary layer very close to the undersurface) parallel flow exists. The configuration is shown in Fig.1, where OBC is the plane shock and triangles OAB and OAC constitute the undersurface. The typical path of an air particle is shown. Fig.2 is the side elevation of the same configuration. In all the calculations which follow it is assumed that the upper surface is in the free stream direction so that the static pressure along the upper surface is the static pressure of the mainstream or, if not in the free stream direction, it is still assumed that $p \sim p_\infty$ so that it will have negligible effect on lift and drag. The configuration considered may only be part of a complete aircraft, anyway. A review of available work on Caret wings is contained in Ref.3.

In supersonic flow past a flat plate at incidence the shock is generally curved at the leading edge due to the displacement effect of the boundary layer, though it soon becomes nearly parallel to the plane predicted for inviscid flow. There are also large changes in pressure near to the leading edge. These effects must always occur but they are probably confined in most cases to a very small region close to the leading edge, and are initially ignored in this study. After performing the calculations on this basis, this assumption can be checked and it is estimated that in most cases leading edge effects are negligible except possibly at very high altitudes, of the order of 300,000 ft, where the density of the air is very small. In such cases our assumption of constant pressure behind the shock is no longer valid. The leading edge effect in most cases may simply be to cause the shock to stand off slightly from the plane OBC.

Once the air has passed through the shock and is assumed to flow parallel to the surface, the flow on each of the two surfaces is similar to that past a swept flat plate edge on to the stream together with some corner effect due to the interaction between the two parts. Gersten[4] has shown that the interference from a corner when two flat plates are inclined at a right angle is such as to displace the flow near the corner by an additional amount comparable in magnitude to the displacement thickness of a single flat plate. It has been shown that this corner effect decreases with increasing Mach number and also decreases as the angle between the plates is increased. In the examples considered in this paper the angle between the plates is $133{\cdot}4^\circ$ and so the corner effect, which is small even when the plates are inclined at a right angle, will be smaller still in our case.

One effect which may be serious, however, was found by Gersten[4], who showed that the corner will cause an earlier transition to turbulence in its neighbourhood than that which occurs on a single flat plate; it is thus possible that there may be a turbulent boundary layer in the region of the ridge. We shall, however, assume laminar flow everywhere and that the flow behaves entirely like two dimensional flow past a flat plate. Gersten[4] shows in fact that the effect of the corner on skin friction drag is very small.

Monaghan[5] shows that when heat is transferred from the free stream to the surface, the critical Reynolds number affecting transition to turbulence is increased considerably and in all the calculations performed here the Reynolds numbers are sub-critical when compared with his results. The laminar flow assumption, therefore, may be expected to give reasonable results.

The Prandtl number, σ, ratio of specific heats, γ, and the specific heat at constant pressure, c_p, are taken as constants and dissociation of the air is neglected.

Flat-plate laminar boundary-layer theory is now used to estimate velocity and temperature fields etc., on the assumption that shock-wave boundary layer interaction at the leading edge has a negligible effect on all the physical quantities calculated. These results will then be used to assess the justification for making this assumption.

2 OBLIQUE SHOCK RELATIONS

With the notation of Figs.1 and 2 and using subscripts ∞ for the free stream and 1 for quantities behind the shock, we have from Ref.6 the following equations:-

$$M_\infty^2 = \frac{4 \operatorname{cosec} 2\zeta}{(\gamma+1)\tan\omega - (\gamma-1)\tan\zeta}, \qquad (1)$$

the condition for a plane attached shock,

$$\frac{\rho_1}{\rho_\infty} = \frac{\tan\zeta}{\tan\omega}, \qquad (2)$$

$$\frac{p_1}{p_\infty} = 1 - \gamma M_\infty^2 \sin^2\zeta \left(\frac{\rho_\infty}{\rho_1} - 1\right), \qquad (3)$$

$$\frac{T_1}{T_\infty} = \frac{p_1}{p_\infty} \times \frac{\rho_\infty}{\rho_1}, \qquad (4)$$

$$\frac{M_1^2}{M_\infty^2} = \frac{p_\infty}{p_1} \frac{\sin 2\zeta}{\sin 2\omega}, \qquad (5)$$

$$\frac{\mu_1}{\mu_\infty} = \left(\frac{T_1}{T_\infty}\right)^{3/2} \frac{T_\infty + S}{T_1 + S}, \qquad (6)$$

and

$$\frac{q_1}{q_\infty} = \frac{\cos \zeta}{\cos \omega} \quad . \tag{7}$$

The pressure coefficient, C_p, is given by

$$C_p = \frac{p_1 - p_\infty}{\frac{1}{2} \rho_\infty q_\infty^2} = \frac{4}{\gamma + 1} \left(\sin^2 \zeta - \frac{1}{M_\infty^2} \right) \quad . \tag{8}$$

Ignoring for the moment contributions from the skin friction the lift and drag coefficients will be respectively

$$C_p \cos \delta \quad \text{and} \quad C_p \sin \delta \tag{9}$$

when based on the area of the projection of triangle OBC on the plane through OA parallel to the deflected flow direction.

3 SKIN FRICTION CONTRIBUTION TO LIFT AND DRAG

Constant Prandtl number, σ, and ratio of specific heats, γ, is assumed and Sutherland's formula (6) for the viscosity is approximated by writing

$$\frac{\mu}{\mu_1} = C \frac{T}{T_1} \quad , \tag{10}$$

where C is a constant evaluated in this case at an "intermediate" temperature as in Eckert's "Intermediate Enthalpy Method" (see Monaghan[5]) with constant c_p. Variations in σ, γ and c_p are shown in Ref.5 to be small in the range of temperatures we are considering. By use of the Howarth[7] transformation the equations for the laminar boundary layer on the undersurface may now be reduced to incompressible form and solved as for a flat plate in a uniform stream. We find that the skin friction τ_o is given by

$$\frac{\tau_o}{\frac{1}{2} \rho_1 q_1^2} = 0{\cdot}664 \sqrt{\frac{C \nu_1}{q_1 x}} \tag{11}$$

where x is measured from the leading edge in the direction of the flow outside the boundary layer.

The drag on the one plate OAB (see Fig.1) is

$$D_f = \int_{z=0}^{AB} dz \int_{x=0}^{x=\ell(1-z/AB)} \tau_o \, dx$$

in the direction $\vec{OA}$, z being measured in a direction parallel to AB, and if we define a skin friction drag coefficient based on the area OAB as $\bar{C}_D = D_f / \frac{1}{2} \rho_\infty q_\infty^2 \cdot \frac{1}{2} \ell \, AB$, where $\ell = OA$, then

$$\bar{C}_D = \frac{\rho_1 q_1^2}{\rho_\infty q_\infty^2} \cdot 1{\cdot}771 \sqrt{\frac{C\nu_1}{q_1 \ell}}$$

$$= 1{\cdot}771 \frac{\sin 2\zeta}{\sin 2\omega} \sqrt{\frac{C}{R_1}} , \qquad (12)$$

where $R_1 = q_1 \ell / \nu_1$, by equations (2) and (7).

If we base our lift and drag coefficients on the projected area of the triangle OBC on the plane through OA parallel to the deflected flow direction, then

$$\left.\begin{aligned} C_L &= C_P \cos\delta - \bar{C}_D \sin\delta / \sin\xi \; ; \\ C_D &= C_P \sin\delta + \bar{C}_D \cos\delta / \sin\xi \; ; \end{aligned}\right\} \qquad (13)$$

and

$$\left.\begin{aligned} L &= \tfrac{1}{2} \rho_\infty q_\infty^2 \, \Delta \, OBC \, C_L \; ; \\ D &= \tfrac{1}{2} \rho_\infty q_\infty^2 \, \Delta \, OBC \, C_D \; , \end{aligned}\right\} \qquad (14)$$

where ξ and δ are defined in Fig.1.

4 HEAT TRANSFER

Eckert's "Intermediate Enthalpy Method" is again used with constant σ, c_p and γ and it is found that the rate at which heat is transferred by diffusion to the surface per unit area is

$$Q = 0{\cdot}4114\, \rho_1\, q_1\, c_p \sqrt{\frac{C}{R_{1x}}}\, (T_{wo} - T_w) \quad ,$$

where $R_{1x} = q_1 x/\nu_1$ and C is again calculated from equation (10) at the "intermediate" temperature (see Ref.5). T_w is the wall temperature and T_{wo} the adiabatic wall temperature, that is, the temperature the wall would attain if there were no heat transfer from the surface:

$$\frac{T_{wo}}{T_1} = 1 + r_T \frac{\gamma - 1}{2} M_1^2 \quad , \tag{15}$$

where $r_T = \sqrt{\sigma}$ for laminar boundary layers.

The rate at which the surface will lose heat by radiation is

$$Q_r = 2{\cdot}78 \times 10^{-12}\, \varepsilon \left(T_w^4 - T_\infty^4 \right) \tag{16}$$

according to the Stefan-Boltzmann Law, where ε is the emissivity factor. If the body were at rest the temperature of the surface would be T_∞ and the amount of heat radiated from the surface per unit time would be $2{\cdot}78 \times 10^{-12}\, \varepsilon\, T_\infty^4$ which must exactly equal the rate at which heat is radiated back from the surrounding air and all other external sources, so that we can consider this quantity to be the rate at which the surface is absorbing heat from all radiating sources external to itself. If the surface is at a temperature T_w different from T_∞ the absorptivity of the surface will change, but this change is very small unless T_w is considerably greater than T_∞. Hence, if T_w is not considerably greater than T_∞ we may regard ε as being constant and the rate at which the surface is absorbing heat from the external radiating sources is $2{\cdot}78 \times 10^{-12}\, \varepsilon\, T_\infty^4$, which accounts for the second term in (16) (see, e.g., Ref.8).

There will also be some heat radiated to the surface by the air, at temperature T_1, between the shock and the surface, but in the examples considered neither the volume of this mass of air, nor its temperature T_1, are high enough to necessitate the inclusion of this source of radiation.

It is supposed that the boundary layer transfers heat to the surface and that some of this is radiated away from the body, but that heat is not conducted away to other parts of the surface or the body.

In such circumstances to effect a heat balance we must have

$$Q = Q_r \quad .$$

An iteration procedure must now be used and by its means T_w may be found to any required accuracy.

The extension to the turbulent case is straightforward but more lengthy.

5 DISPLACEMENT THICKNESS AND TEMPERATURE PROFILE

The following approximations to temperature profile and displacement thickness are given in Ref.9:-

$$\frac{T}{T_1} = A + B\frac{q}{q_1} - \bar{D}\left(\frac{q}{q_1}\right)^2 \quad , \tag{17}$$

$$\frac{1}{2}\frac{y}{x}\sqrt{R_{1x}} = \frac{\sqrt{C}}{0{\cdot}664}\left\{\left(A - \frac{\bar{D}}{2}\right)\sin^{-1}\left(\frac{q}{q_1}\right) + \left(\frac{\bar{D}}{2}\frac{q}{q_1} - B\right)\sqrt{1 - \left(\frac{q}{q_1}\right)^2} + B\right\}, \tag{18}$$

and

$$\frac{1}{2}\frac{\delta^*}{x}\sqrt{R_{1x}} = \frac{\sqrt{C}}{0{\cdot}664}\left\{\left(A - \frac{\bar{D}}{2}\right)\frac{\pi}{2} + B - 1\right\} \quad , \tag{19}$$

where

$$A = \frac{T_w}{T_1} \; ; \quad B = 0{\cdot}89835\left(\frac{T_{wo}}{T_1} - \frac{T_w}{T_1}\right) \; ; \quad \bar{D} = 0{\cdot}145\,M_1^2 \quad . \tag{20}$$

These give fair approximations to temperature profiles up to about $q/q_1 = 0{\cdot}8$. A separate check with exact numerical results from Ref.11 was made and very good agreement was found to exist.

6 DISCUSSION OF RESULTS

All the calculations have been performed on the Ferranti Mercury computer using an emissivity ε of 0·8, an overall length ℓ of 200 ft and an angle ξ (see Fig.1) of 66·7°. This value of ξ was used by Squire[11] for one of his wind tunnel models. The only effect of decreasing ξ (besides

increasing the corner effect as mentioned in the Introduction), for fixed ω, is to decrease the area of the undersurface and so decrease the contribution of the skin friction to C_L and C_D.

Fig.3 shows the effect of incidence on L/D at design conditions for various values of the ridge angle ω at a height of 200,000 ft and Fig.4 the same at 300,000 ft. Fig.5 compares the L/D curve for $\omega = 6^\circ$ from Fig.3 with the L/D curve neglecting skin friction drag, that is L/D = cot δ, from (9). It may be seen that the skin friction drag effect is only appreciable when the incidence (or more particularly flow deflection δ) is small.

Figs.6 and 7 show the relation between Mach number and design incidence for various values of ω, these curves being the same in the two graphs; they also give L/D curves at 200,000 ft and 300,000 ft respectively. The curves of constant ω are curtailed at $\omega = \zeta$ because there the flow is, of course, not deflected so that there will be no shock for $\zeta < \omega$. For any given configuration ω is fixed and it may be noted that, for a given ω, design conditions are only possible if the Mach number is greater than a certain minimum. For example, if $\omega = 5^\circ$ then M_∞ must be greater than 8·79 for design conditions (that is, to ensure that a plane shock will sit on the underside as in Fig.1). The relationship between ω and this minimum value of M_∞, or alternatively between M_∞ and ω_{min} is shown in Fig.8. Returning to Figs.6 and 7, we may note that when M_∞ is near its minimum value there are two values of ζ which will give design conditions, and also in this region, provided ω is not too small, the design Mach number is fairly insensitive to changes in ζ.

If the total mass of the structure and load is WA lb where W is the wing loading and A/cos ω the area of triangle OBC, and the lift generated by the propulsion system is PA, then in order to cruise at a fixed altitude the aerodynamic lift coefficient must satisfy the relation

$$(WA - PA)g = \tfrac{1}{2}\rho_\infty q_\infty^2 A C_L g + WA\, q_\infty^2/R \quad , \tag{21}$$

where R is the radius of the earth, neglecting the increment from the height above sea level, and the last term represents the contribution to the lift from orbital centrifugal forces.

When P = 0,

$$C_L = \frac{2W}{\rho_\infty}\left[\frac{1}{a_\infty^2 M_\infty^2} - \frac{1}{Rg}\right] . \tag{22}$$

Fig.9 shows altitude against Mach number for fixed values of C_L calculated from (22) (the broken lines) when W = 75 lb/ft^2. R is taken as 4000 miles. The values of C_L used are 2·212, 0·553, 0·246, 0·138 and 0·0885 and these correspond, when M_∞ is small so that orbital effects may be neglected,

to equivalent air speeds of 100, 200, 300, 400 and 500 knots respectively. The equivalent air speed v_o is obtained from the formula $\frac{1}{2} \rho_\infty q_\infty^2 = \frac{1}{2} \rho_o v_o^2$ where ρ_o is the density at sea level, so that for small Mach numbers $C_L = 2 W/\rho_o v_o^2$.

It has been suggested that to fly slower than about 200 knots or faster than about 400 knots equivalent air speeds would be impracticable from considerations of the extra structure/engine weight needed for high speeds and the high lift that would have to be generated for low speeds. The heavy lines in Fig.9 correspond to equivalent air speeds of 200 and 400 knots for low Mach numbers and so a feasible cruising region exists between them. For a given Caret wing configuration at a given height the lift coefficient will depend on the Mach number, and where this C_L is equal to the C_L calculated from (22) at the same Mach number the configuration will be able to cruise at this height with a wing loading of W. Fig.9 also shows altitude against Mach number for various values of ω under cruising conditions when the wing loading is $W = 75$ lb/ft^2, assuming no contribution to the lift from the propulsion system. It may be noted that wide ranges of Mach number and altitude within the feasible cruising corridor can only be realised if ω is between about 5° and 8°, but to fly at lower altitudes and Mach numbers within this corridor ω will have to be much higher. Viscous effects are included, but are small.

In most cases the displacement thickness of the boundary layer is very small compared with the distance from the shock to the undersurface. Very near the leading edge, however, these distances become comparable and the displacement surface actually appears on the outside of the assumed shock position. This is shown in Fig.10 which depicts the rear section (see Fig.1), although the actual case shown is a very extreme one, where δ^* is large. δ^* becomes large only when the shock turning angle, δ, is very small so that the shock will be weak and the density of the air will not increase by a great amount on passing through the shock. For the case shown $\delta = \zeta - \beta = 1{\cdot}05^\circ$.

Since δ^* is approximately proportional to $x/\sqrt{R_{1x}}$ where

$$R_{1x} = \frac{q_1 x}{\nu_1} = \frac{q_1 \rho_1 x}{\mu_1} ,$$

x being the distance from the leading edge measured parallel to the stream, then δ^* will decrease as the altitude decreases, because of the rapid increase in density with decreasing altitude. For example, for the configuration shown in Fig.10 the displacement thickness at a distance of 200 ft from the leading edge is 0·95 ft at an altitude of 200,000 ft compared with 9 ft at 300,000 ft, the case shown in the figure. The calculations have taken no account of the corner at A and a slight thickening of the boundary layer may be expected there. When the displacement thickness becomes large, as in Fig.10, the assumed flow model becomes unrealistic; the shock will in fact be displaced outwards at the leading edge and stand off slightly and it may be necessary

to use more refined methods of calculation. In the vast majority of cases, in fact in all the cases considered at an altitude of 200,000 ft or less, the boundary layer may be concluded to have a negligible effect on the shape of the shock except in a very small region near the leading edge. In calculating the inviscid flow behind the shock the 'effective' body is now the displacement surface. When δ^* is small the deviation from parallel inviscid flow will be very small. Strictly speaking ω will be the angle between the shock and the displacement surface. This surface is not, of course, plane but we can roughly calculate the true ridge angle, knowing δ^* at the trailing edge, if we take the line through the leading edge, parallel to the flow direction, which cuts the displacement surface at the trailing edge as being representative of this surface. In most cases the true ridge angle was found to be within one per cent of the assumed ω.

Near to the leading edge there are large changes of pressure and our calculations are invalidated here, since we have assumed zero pressure gradient. However, this region of high pressure gradient is small, and, from Ref.12, may be estimated in most cases to extend a distance of about 0·1 ft downstream provided the incidence is not small. After this our calculations may be expected to be valid.

Fig.11 gives velocity and temperature profiles calculated from equations (17) to (20) for the same configuration as in Fig.10, but at an altitude of 200,000 ft, at distances from the leading edge, measured in the stream direction, of 1, 10, 100 and 200 ft. Equations (17) to (20) are shown in Ref.10 to give fair approximations up to about $q/q_1 = 0{\cdot}8$. The broken lines in Fig.11 show where the graphs have been extrapolated beyond this. Radiation of heat plays an important part in the determination of temperature and Fig.11 shows that, except very near the leading edge, the surface temperatures are not so high as perhaps might have been expected. Thus even at 1 ft behind the leading edge the temperature in the example shown is only 650°K whilst the zero heat transfer temperature T_{wo} is 3760°K. The surface temperature drops to 360°K at 200 ft from the leading edge. Inside the boundary layer the temperatures rise to much higher values, having maxima of 1150°K at 200 ft and 1300°K at 1 ft from the leading edge. An emissivity factor of 0·8 has been assumed. It will obviously be important to keep this as high as possible and it will also be very necessary to ensure that the boundary layer remains laminar.

Conduction of heat into the body or along the surface has been neglected, so that actually the temperature of the surface will be more evenly distributed and temperatures near the rear will be slightly higher than those given.

Fig.12 shows the temperatures which may be encountered in an actual flight. The temperatures are those of the surface 200 ft from the leading edge and the curves correspond to the flight paths shown in Fig.9. The flight corridor depicted in Fig.9 will exclude all the high values of T_w near ground level.

Fig.13 shows wall temperatures plotted against distance from leading edge taken at positions along the flight path for $\omega = 6^\circ$ from Fig.9. At the leading edge the temperature reaches the adiabatic wall temperature T_{wo} and these temperatures are shown opposite arrows on the three curves shown. Although the first of these curves may at first sight seem to be at variance with Fig.11 in that it gives a higher temperature at the trailing edge and a lower one at the leading edge this is quite consistent and is explained by the fact that in Fig.11 the Mach number after passing through the shock is higher since the shock is weak and this increases the adiabatic wall temperature, while the temperature behind the shock is lower, so lowering the trailing edge temperature.

The variation of displacement thickness along one of the flight paths is shown in Fig.14 which gives the displacement thickness 200 ft from the leading edge of a configuration with a ridge angle of 7°. The very rapid increase in δ^* above about 200,000 ft is very noticeable in this graph. Also shown in Fig.14 is the variation in incidence along the same flight path.

7 CONCLUSIONS

Flat plate boundary layer theory has been used to give some idea of the velocity and temperature fields on the undersurface of a Caret wing configuration and to estimate the effect of the skin friction on lift and drag coefficients. It is found that in most cases, except at high altitudes where the density is low, the boundary layer will have a negligible effect on the shape of the shock lying beneath the configuration but that when the incidence is low the skin friction has a considerable effect on the lift/drag ratio. For low incidences and altitudes above 200,000 ft the method breaks down and it is suggested that wind-tunnel experiments would be needed to obtain a picture of the flow in these cases.

ACKNOWLEDGEMENT

The author wishes to thank Professor J.C. Cooke for the many helpful discussions conducted during the preparation of this Note.

LIST OF SYMBOLS

a	velocity of sound (ft/sec)	
A	$\frac{T_w}{T_1}$	(section 5)
B	$0{\cdot}89835 \left(\frac{T_{wo}}{T_1} - \frac{T_w}{T_1}\right)$	(section 5)
$\bar{D}$	$0{\cdot}145\ M_1^2$	(section 5)
C	constant appearing in $\frac{\mu}{\mu_1} = C\ \frac{T}{T_1}$	
$\bar{C}_D$	skin friction drag coefficient	
C_D	drag coefficient	
C_L	lift coefficient	
C_P	pressure coefficient	
c_p	specific heat at constant pressure (C.H.U.ft/sec^2 lb °K) = 7·73	
D	drag (lb)	
L	lift (lb)	
ℓ	length of ridge line OA (ft)	
M	Mach number	
p	pressure (lb/ft^2)	
q	velocity (ft/sec)	
Q	heat transferred by diffusion to surface per unit time per unit area (C.H.U./ft^2 sec)	
Q_r	net heat radiated from surface per unit time per unit area (C.H.U./ft^2 sec)	
R	earth's radius	
R with subscript	Reynolds number	

LIST OF SYMBOLS (Contd)

r_T temperature recovery factor

S Sutherland's constant taken to be 114°K

T temperature (°K)

T_{wo} adiabatic wall temperature

W wing loading (lb/ft^2)

x distance along flat plate from leading edge (ft)

γ ratio of specific heats = 1·4 for air

δ^* displacement thickness (ft)

δ flow turning angle = $\zeta - \beta$

ε emissivity

ζ shock angle = design incidence

μ coefficient of viscosity (lb sec/ft^2)

ν kinematic viscosity (ft^2/sec) = μ/ρ

ξ the angle BAX, complementary to the anhedral (see Fig.1)

ρ density (lb sec^2/ft^4)

σ Prandtl number = 0·725

τ_o skin friction

ω ridge angle = angle between shock and undersurface ridge-line

Subscripts

∞ free stream

1 behind shock but outside boundary layer

w wall (i.e. undersurface)

LIST OF REFERENCES

No.	Author(s)	Title, etc
1	Nonweiler, T.R.F.	Delta wings of shapes amenable to exact shock wave theory. A.R.C. 22,644, March 1961.
2	Maikopar, G.I.	On the wave drag of axisymmetric bodies at supersonic speeds. Russian Journal of Applied Mathematics and Mechanics (Pergamon translation) 23 (2), 1959, 528-531.
3	Peckham, D.H.	On three dimensional bodies of delta planform which can support plane attached shock waves. A.R.C. C.P.640. March, 1962.
4	Gersten, K.	Corner interference effects. A.G.A.R.D. Report 299, March 1959.
5	Monaghan, R.J.	Formulae and approximations for aerodynamic heating rates in high speed flight. A.R.C. C.P.360. October, 1955.
6	Howarth, L. (Ed.)	Modern developments in fluid dynamics - High speed flow (Oxford University Press) Vol.1, p.111, 1953.
7	Howarth, L.	Concerning the effects of compressibility on laminar boundary layers and their separation. Proc. Roy. Soc. A, 194, 1948, p16.
8	Starling, S.G., Woodall, A.J.	Physics (Longmans) pp 345-6, 1957.
9	Monaghan, R.J.	An approximate solution of the compressible laminar boundary layer on a flat plate. A.R.C. R. & M. 2760, November, 1949.
10	Van Driest, E.R.	Investigation of laminar boundary layer in compressible fluids using the Crocco method. NACA-TN-2597, January 1952.

LIST OF REFERENCES (Contd)

No.	Author(s)	Title, etc
11	Squire, L.C.	Pressure distributions and flow patterns at M = 4·0 on some delta wings of inverted 'V' cross-section. R.A.E. Tech Note Aero 2838. A.R.C. 24,449. August, 1962.
12	Cheng, H.K. et al	Boundary-layer displacement and leading-edge bluntness effects in high-temperature hypersonic flow. J.Aero/Space Sci 28 (5) May 1961.

WT.2078 C.P.694 K3. Printed in England.

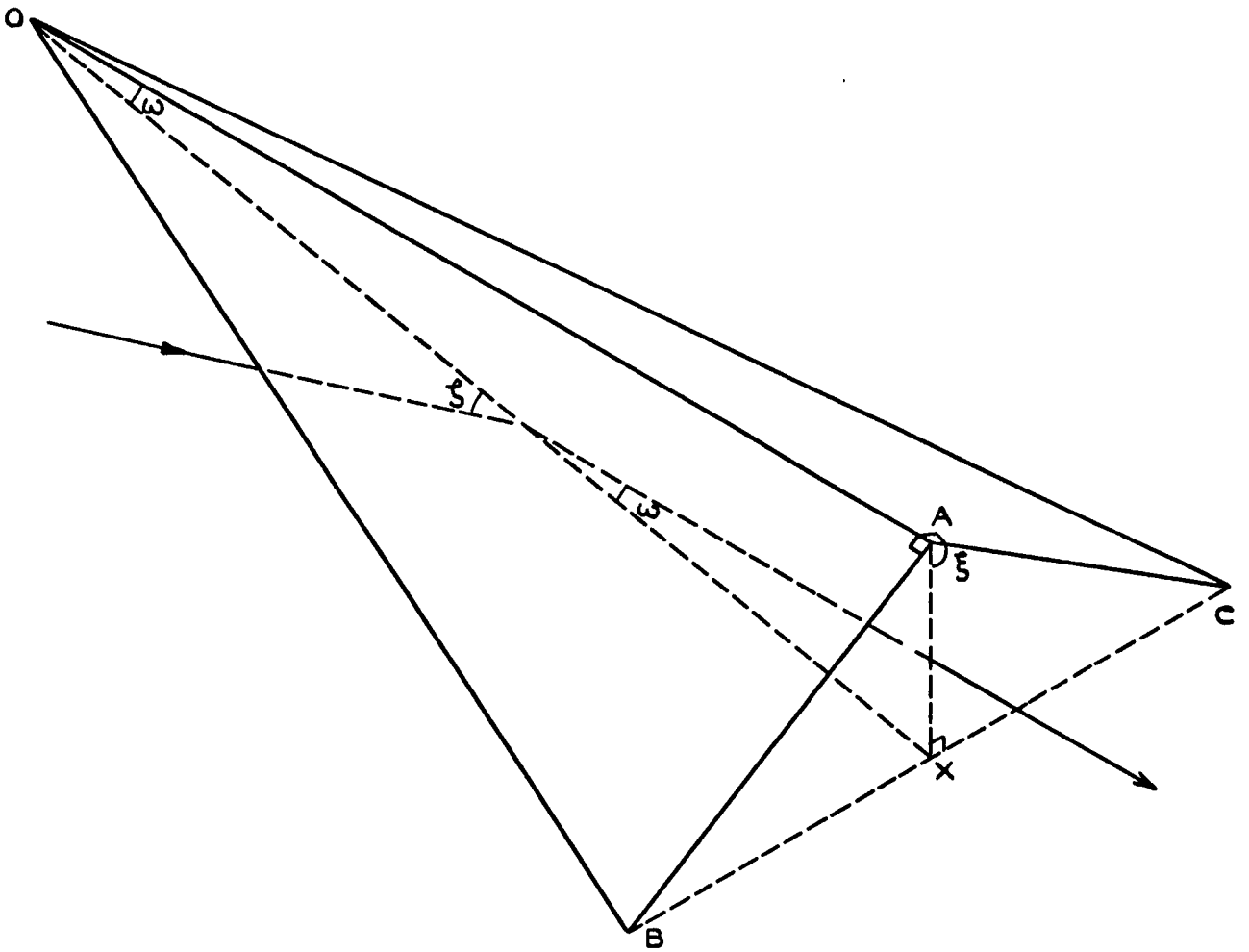

FIG. 1. CARET WING.
ISOMETRIC VIEW

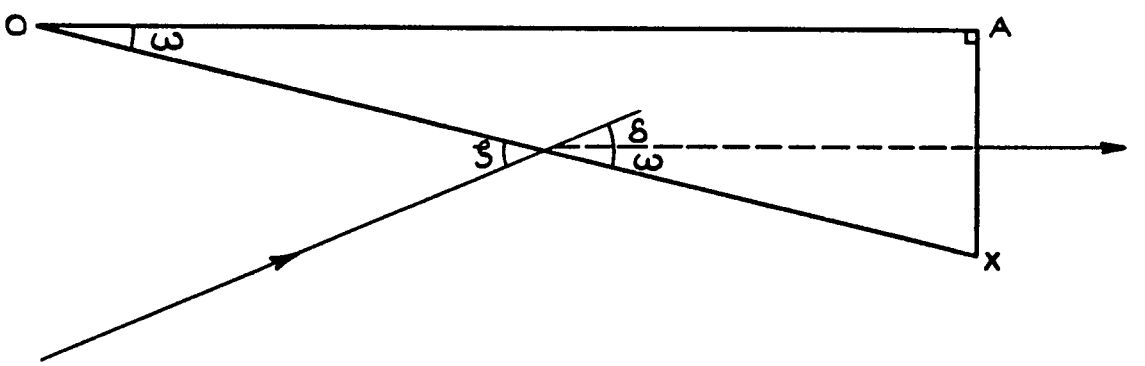

FIG. 2. CARET WING.
SIDE ELEVATION

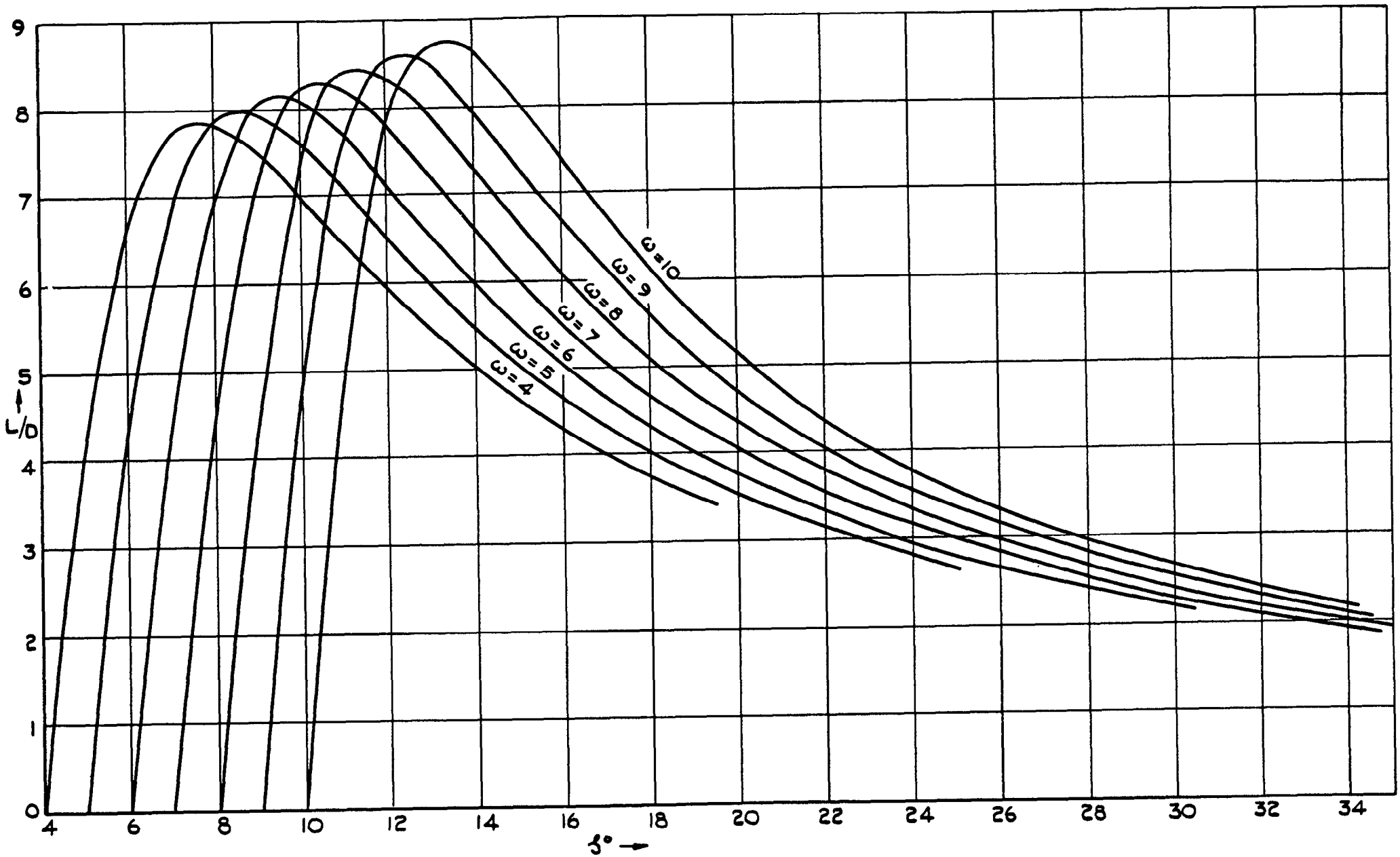

FIG. 3. L/D AGAINST INCIDENCE FOR VARIOUS RIDGE ANGLES AT HEIGHT 200,000 FT., ℓ = 200 FT., $\S$ = 66·7°, ε = 0·8.

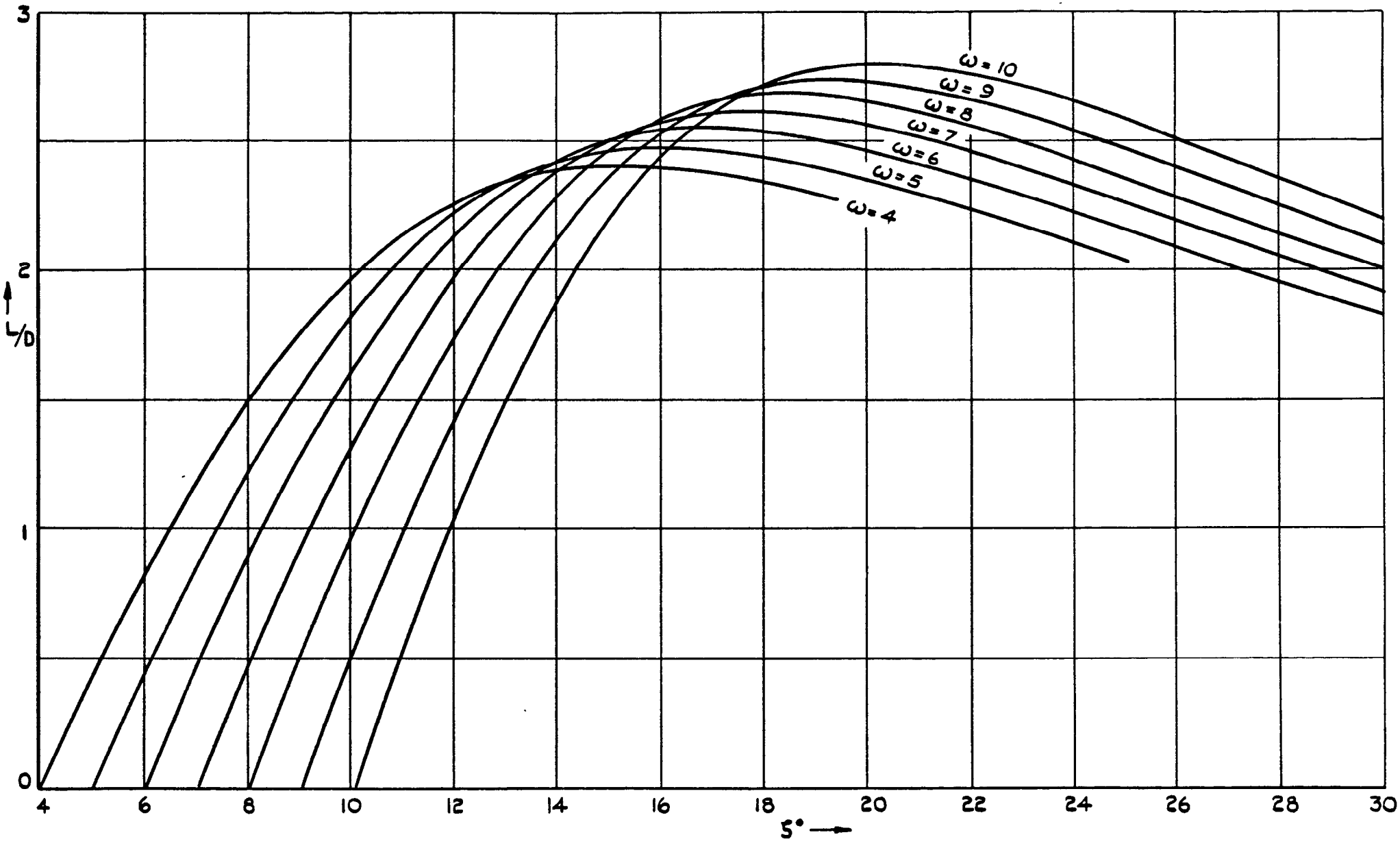

FIG.4. L/D AGAINST INCIDENCE FOR VARIOUS RIDGE ANGLES AT HEIGHT 300,000 FT., ℓ = 200 FT., ξ = 66·7°, ε = 0·8.

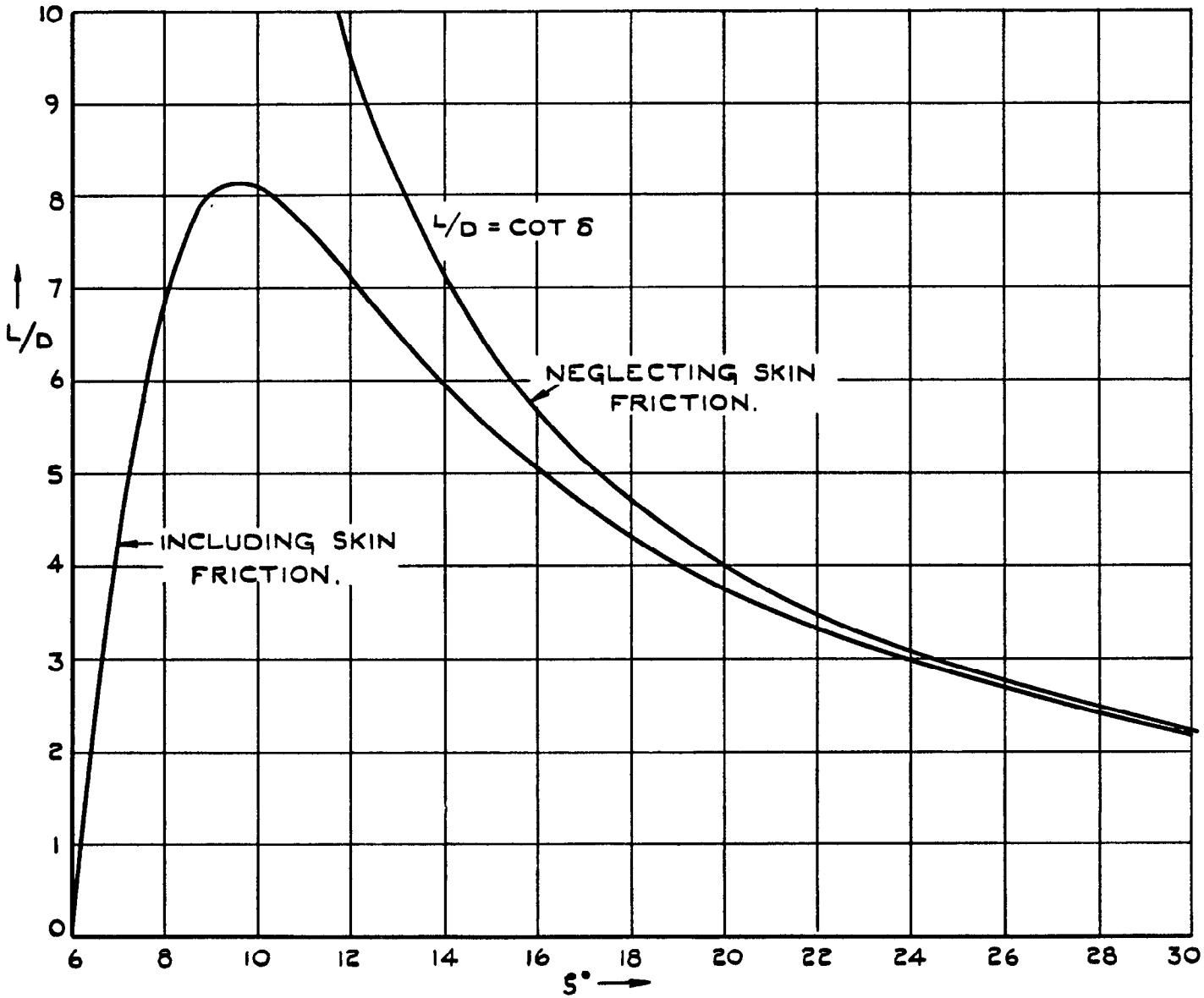

FIG. 5. L/D AGAINST INCIDENCE AT HEIGHT 200,000FT. $\omega = 6°$, $\ell = 200$FT., $\xi = 66{\cdot}7°$, $\varepsilon = 0{\cdot}8$ AND L/D AGAINST INCIDENCE NEGLECTING SKIN FRICTION WHEN $\omega = 6°$.

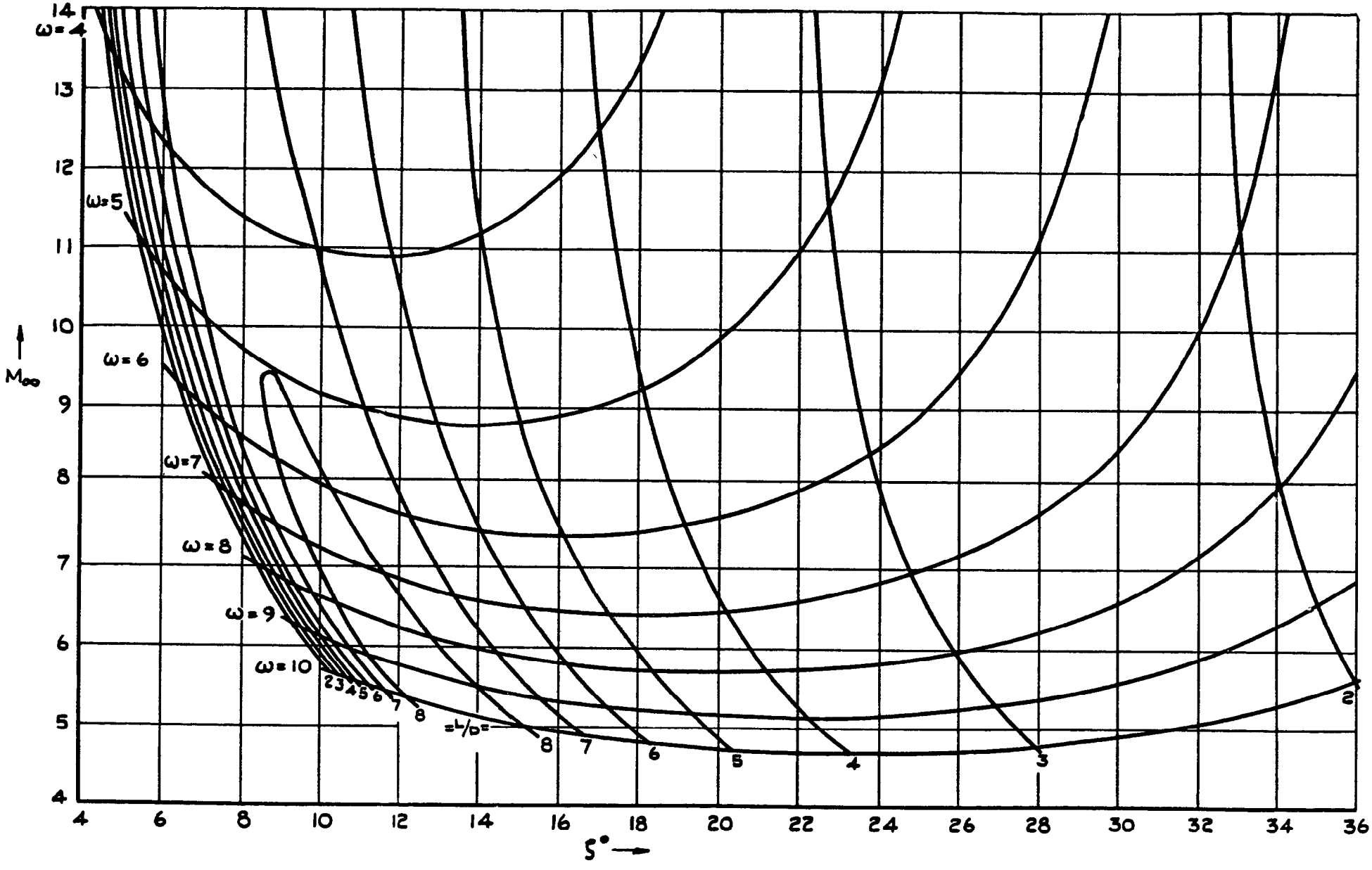

FIG. 6. MACH No. AGAINST INCIDENCE FOR VARIOUS RIDGE ANGLES AND L/Ds AT HEIGHT 200,000 FT., ℓ = 200 FT., ξ = 66·7°, ε = 0·8.

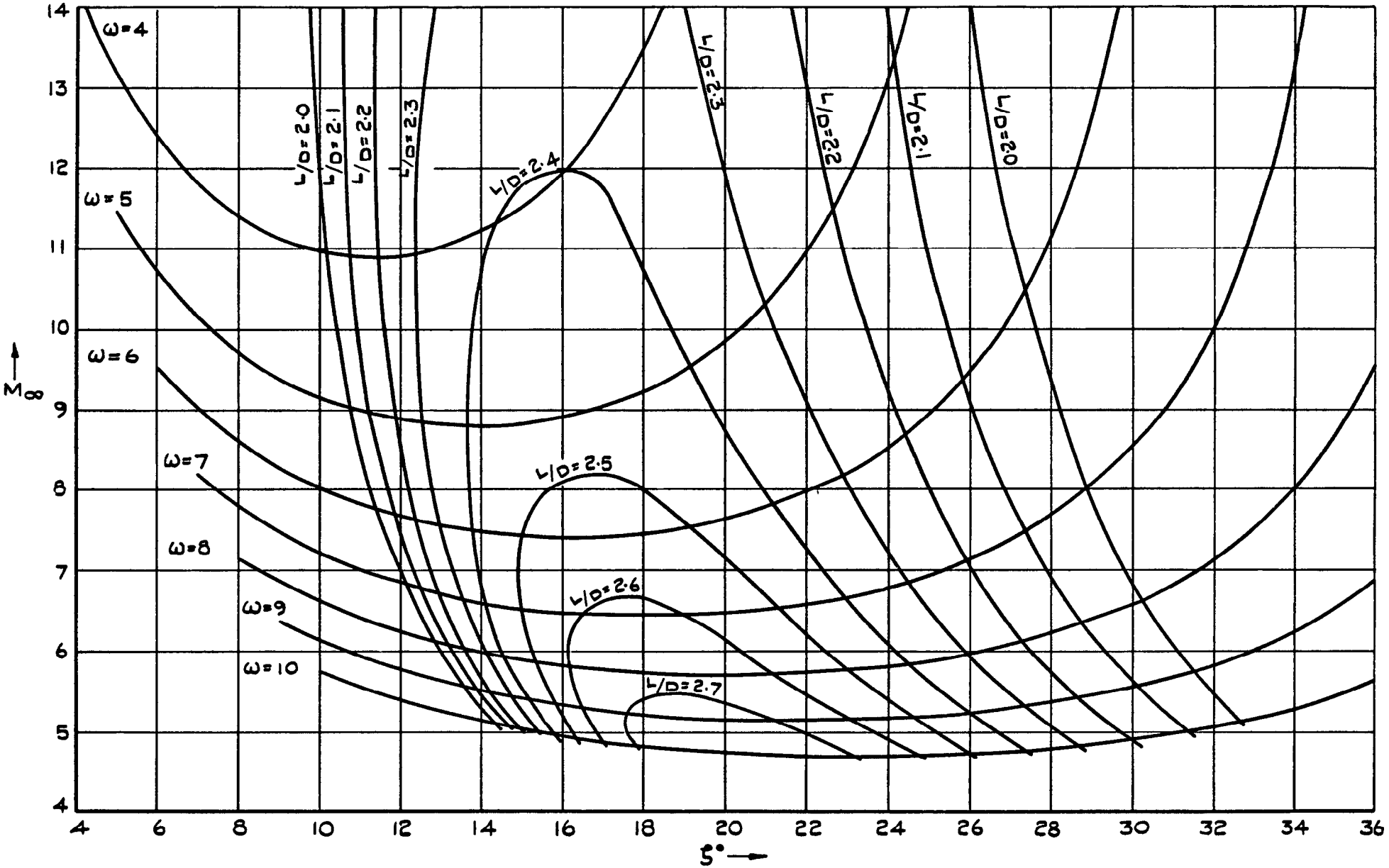

FIG.7. MACH No. AGAINST INCIDENCE FOR VARIOUS RIDGE ANGLES AND L/Ds AT HEIGHT 300,000 FT., ℓ = 200 FT., ξ = 66·7°, ε = 0·8.

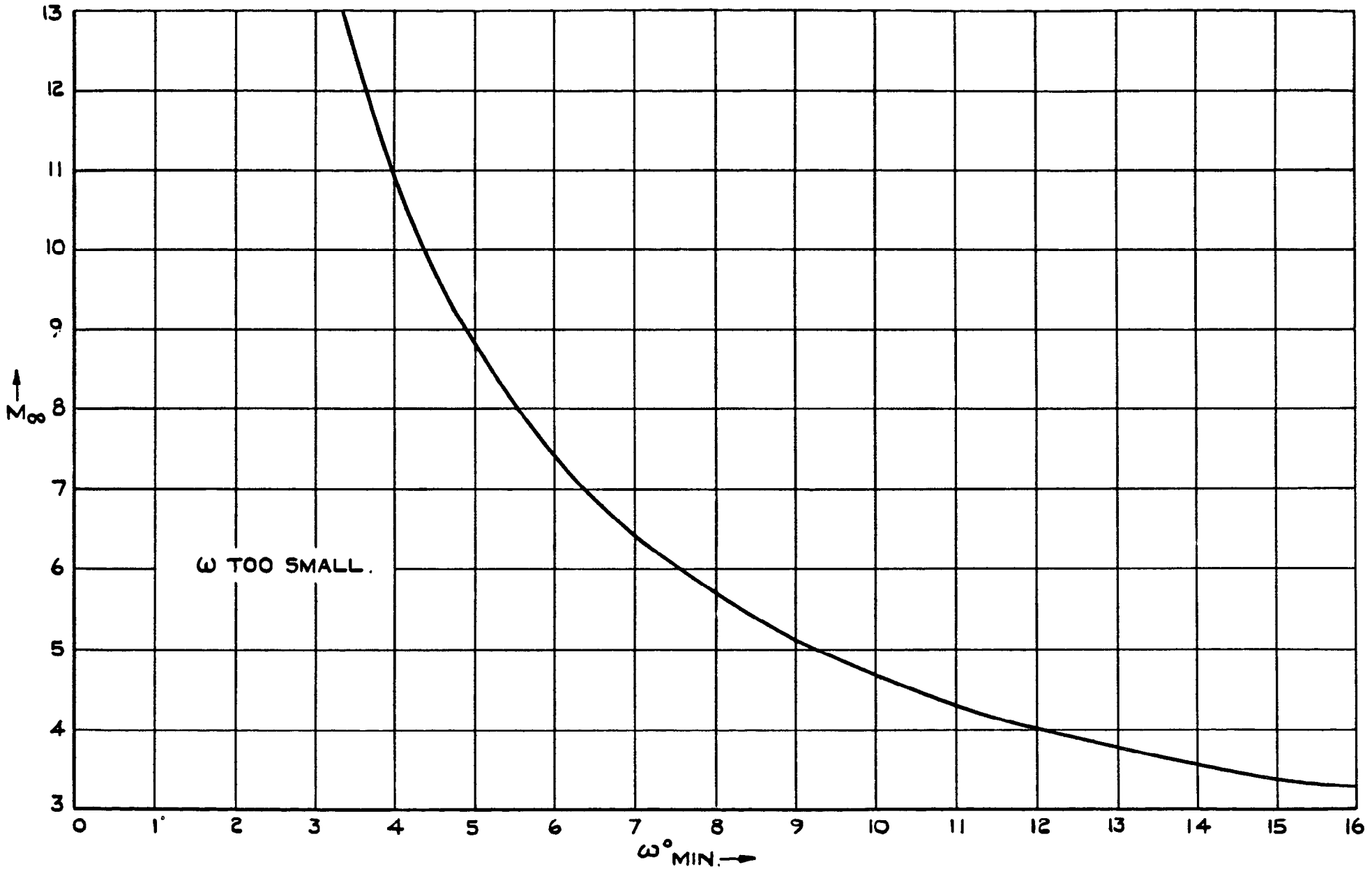

FIG. 8. MINIMUM VALUES OF RIDGE ANGLE FOR DESIGN CONDITIONS.

Published by
HER MAJESTY'S STATIONERY OFFICE

To be purchased from
York House, Kingsway, London W.C.2
423 Oxford Street, London W.1
13A Castle Street, Edinburgh 2
109 St. Mary Street, Cardiff
39 King Street, Manchester 2
50 Fairfax Street, Bristol 1
35 Smallbrook, Ringway, Birmingham 5
80 Chichester Street, Belfast 1
or through any bookseller

S.O. CODE No. 23-9013-94

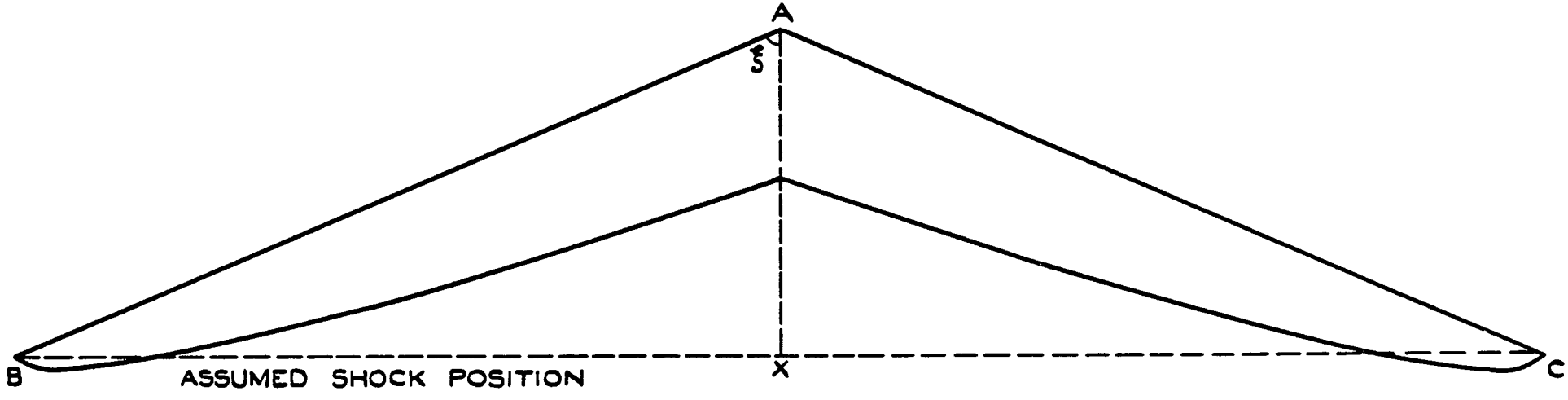

FIG. 10. REAR SECTION SHOWING DISPLACEMENT THICKNESS. $\omega = 6^\circ$, $M_\infty = 9$, $\xi = 7{\cdot}05^\circ$
HEIGHT 300,000FT., $\varepsilon = 0{\cdot}8$, $\xi = 66{\cdot}7^\circ$, $\ell = 200$FT.

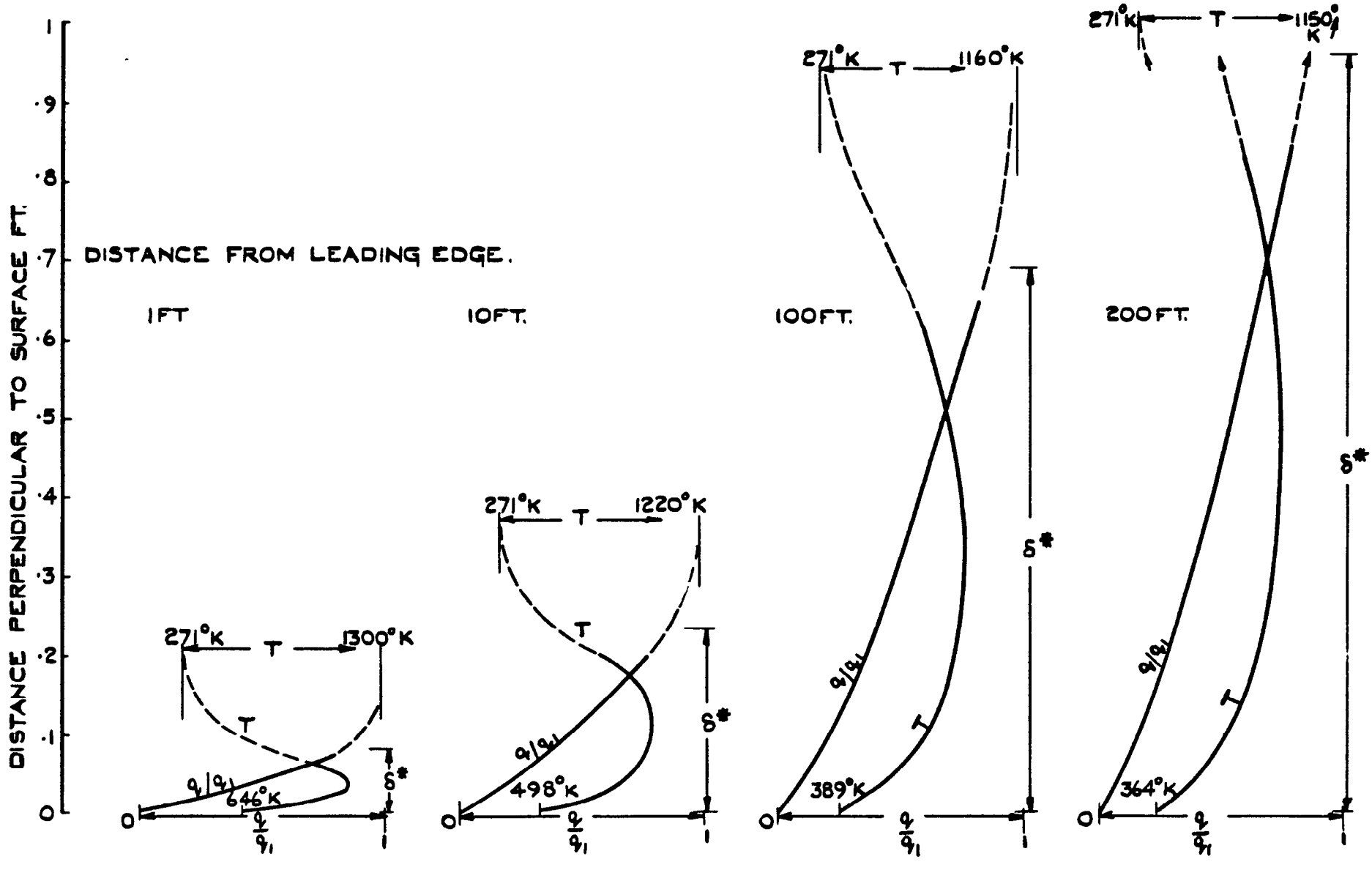

FIG. 11. VELOCITY AND TEMPERATURE PROFILES AT HEIGHT 200,000FT.
$\omega = 6^{\circ}$, $M_{\infty} = 9$, $\zeta = 7 \cdot 05^{\circ}$, $\varepsilon = 0 \cdot 8$.

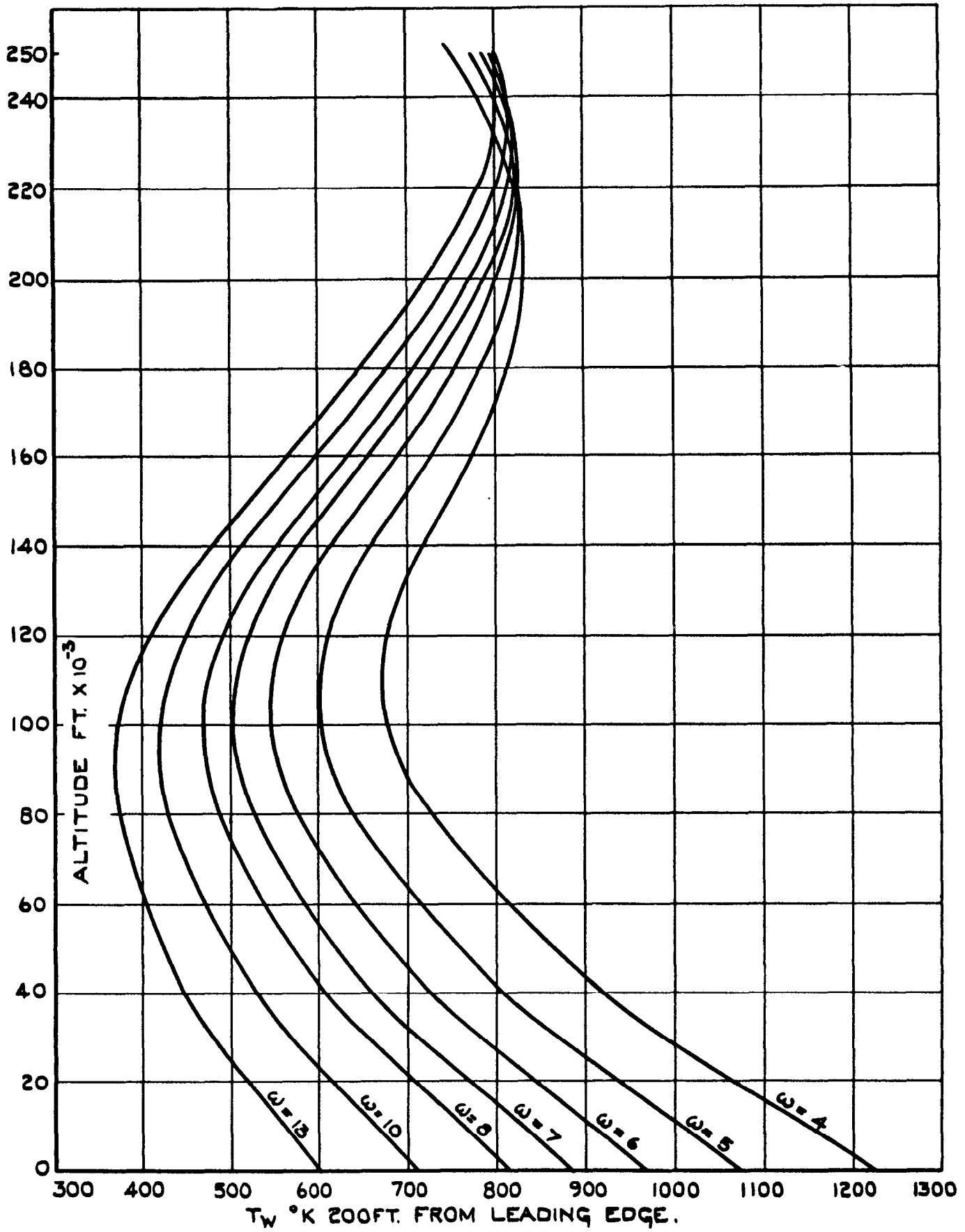

FIG. 12. ALTITUDE AGAINST MINIMUM SURFACE TEMPERATURE ALONG FLIGHT PATHS FOR VARIOUS RIDGE ANGLES. $\xi = 66{\cdot}7^{\circ}$, $\varepsilon = 0{\cdot}8$ WING LOADING 75Lb./FT.^{2}.

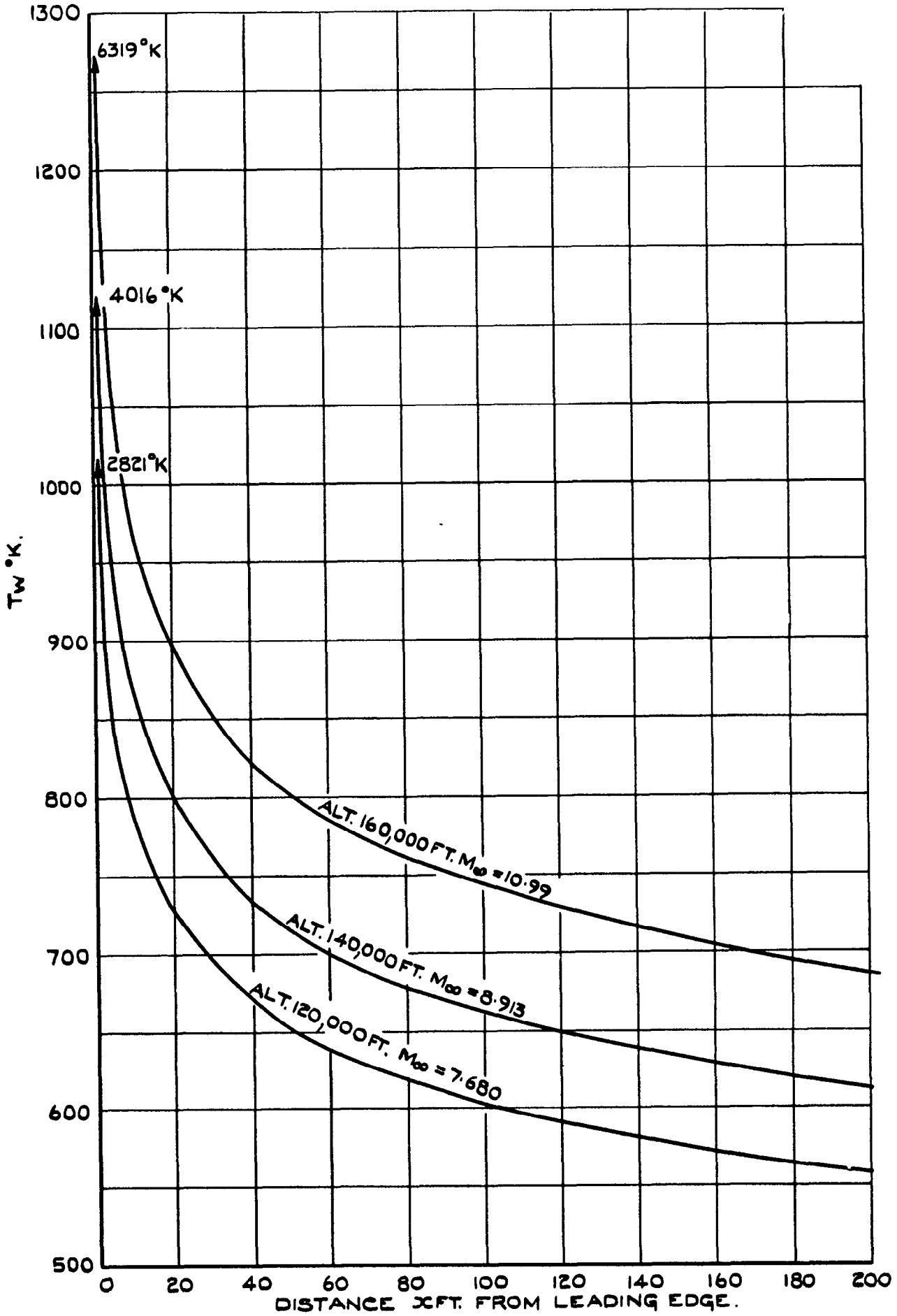

FIG. 13. WALL TEMPERATURE AGAINST DISTANCE FROM LEADING EDGE FOR $\omega = 6°$ AT POSITIONS ON FLIGHT PATH. $\varepsilon = 0 \cdot 8$.

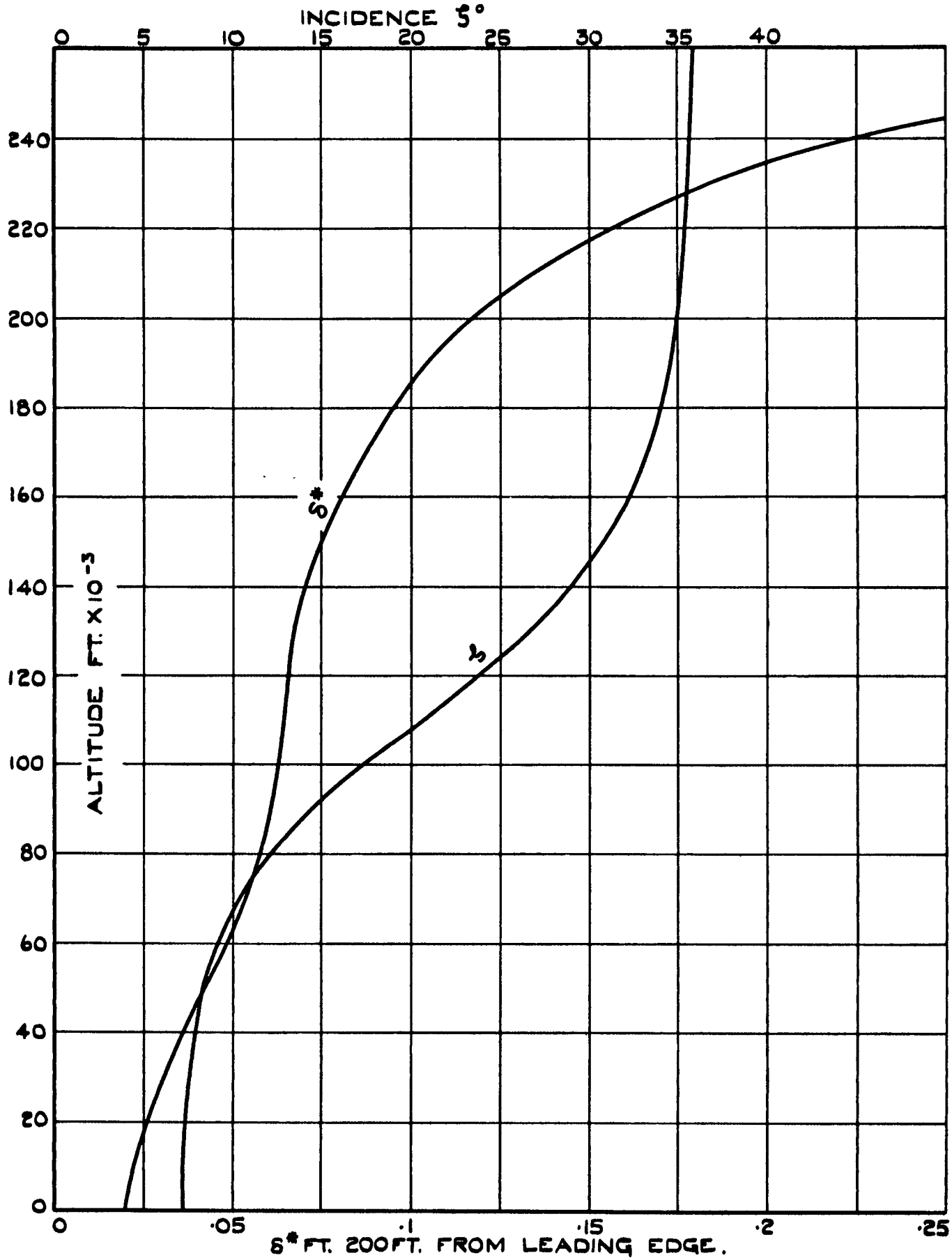

FIG. 14. ALTITUDE AGAINST MAXIMUM DISPLACEMENT THICKNESS AND INCIDENCE ALONG FLIGHT PATH FROM FIG. 9. FOR $\omega = 7°$, $\xi = 66 \cdot 7°$, $\varepsilon = 0 \cdot 8$ WING LOADING 75 LBS./FT.^{2} $\ell = 200$FT.

A.R.C. C.P. No.694 533.693.3 : 532.526

BOUNDARY LAYER CHARACTERISTICS OF CARET WINGS. Catherall, D. May, 1963.

The theory of laminar boundary layers along flat surfaces has been used in conjunction with Eckert's "Intermediate Enthalpy" method to obtain approximations to the displacement thickness, skin friction and temperature profiles on the undersurface of a Caret wing configuration. To a first approximation it has been assumed that parallel flow exists behind the shock outside the boundary layer, and the displacement of the shock by the boundary layer near the leading edge is neglected.

Conduction of heat within the body and along the surface is neglected, but radiation is included, so that 'local' values of equilibrium temperature are found. Examples are given for various altitudes and configurations and the effect of the skin friction on the lift/drag ratio calculated, assuming the undersurfaces to be plane.

A.R.C. C.P. No.694 533.693.3 : 532.526

BOUNDARY LAYER CHARACTERISTICS OF CARET WINGS. Catherall, D. May, 1963.

The theory of laminar boundary layers along flat surfaces has been used in conjunction with Eckert's "Intermediate Enthalpy" method to obtain approximations to the displacement thickness, skin friction and temperature profiles on the undersurface of a Caret wing configuration. To a first approximation it has been assumed that parallel flow exists behind the shock outside the boundary layer, and the displacement of the shock by the boundary layer near the leading edge is neglected.

Conduction of heat within the body and along the surface is neglected, but radiation is included, so that 'local' values of equilibrium temperature are found. Examples are given for various altitudes and configurations and the effect of the skin friction on the lift/drag ratio calculated, assuming the undersurfaces to be plane.

A.R.C. C.P. No.694 533.693.3 : 532.526

BOUNDARY LAYER CHARACTERISTICS OF CARET WINGS. Catherall, D. May, 1963.

The theory of laminar boundary layers along flat surfaces has been used in conjunction with Eckert's "Intermediate Enthalpy" method to obtain approximations to the displacement thickness, skin friction and temperature profiles on the undersurface of a Caret wing configuration. To a first approximation it has been assumed that parallel flow exists behind the shock outside the boundary layer, and the displacement of the shock by the boundary layer near the leading edge is neglected.

Conduction of heat within the body and along the surface is neglected, but radiation is included, so that 'local' values of equilibrium temperature are found. Examples are given for various altitudes and configurations and the effect of the skin friction on the lift/drag ratio calculated, assuming the undersurfaces to be plane.

Published by
HER MAJESTY'S STATIONERY OFFICE

To be purchased from
York House, Kingsway, London W.C.2
423 Oxford Street, London W.1
13A Castle Street, Edinburgh 2
109 St. Mary Street, Cardiff
39 King Street, Manchester 2
50 Fairfax Street, Bristol 1
35 Smallbrook, Ringway, Birmingham 5
80 Chichester Street, Belfast 1
or through any bookseller

S.O. CODE No. 23-9013-94